Desalination and Water Treatment
www.deswater.com
doi: 10.1080/19443994.2014.957931

55 (2015) 3231–3240
September

Taylor & Francis
Taylor & Francis Group

Design of Permeable Adsorptive Barriers (PABs) for groundwater remediation by COMSOL Multi-physics simulations

I. Bortone[a,*], A. Erto[b], G. Santonastaso[a], A. Di Nardo[a], M. Di Natale[a], D. Musmarra[a]

[a]*Dipartimento di Ingegneria Civile, Design, Edilizia e Ambiente, Seconda Università degli Studi di Napoli, via Roma 29, 81031 Aversa (CE), Italy, email: immacolata.bortone@unina2.it (I. Bortone)*
[b]*Dipartimento di Ingegneria Chimica, dei Materiali e della Produzione Industriale, Università degli Studi di Napoli Federico II, P.le Tecchio 80, 80125 Napoli, Italy*

Received 28 April 2014; Accepted 16 June 2014

ABSTRACT

This work deals with an innovative approach to design a permeable reactive barrier (PRB) filled with activated carbon, namely a permeable adsorptive barrier (PAB). A 2D numerical model, solved using a finite element approach via COMSOL Multi-physics, was used to describe the pollutant transport within groundwater and the pollutant adsorption onto the barrier. The PAB design procedure was applied to a benzene-contaminated aquifer situated in the metropolitan area of North Naples (Italy), lately hit the headlines as "Gomorra's land". Model results showed that PAB is an effective tool for the remediation of the aquifer under analysis, since the pollutant concentration downstream the barrier resulted everywhere lower than the regulatory limit set for groundwater. A sensitivity analysis was carried out to evaluate the influence of some site parameters on the PAB design, i.e. hydraulic conductivity and dispersivity. Finally, the simulation results allow estimating the long-term efficiency of the treatment system and the time required to achieve a complete restoration of the aquifer.

Keywords: PRB; Groundwater protection; Aquifer remediation; Adsorption; Benzene

1. Introduction

Groundwater pollution due to contaminant seepage from the disposal sites is a widespread concern in many countries [1]. Organic compounds such as BTEX (benzene, toluene, etc.) are among the most frequently detected groundwater contaminants, also defined as priority pollutants by USEPA [2–4]. In particular, benzene is considered as a major treat for water resources as it is the most water soluble BTEX and because it is carcinogenic [5]. It has been identified in at least 1,000 of the 1,684 hazardous waste sites proposed for inclusion in the EPA National Priorities List [6,7]. The main source of benzene releases in groundwater is due to human activities; it can be released to water from gasoline leaks from underground storage tanks, accidental spills during transportation of chemical products, discharges of untreated industrial wastewater and from landfill and other contaminated soil leachate [8,9].

*Corresponding author.

Presented at the Conference on Desalination for the Environment: Clean Water and Energy 11–15 May 2014, Limassol, Cyprus

The most relevant reactive processes used to decontaminate groundwater from organic compounds include physical, biological and chemical treatments [10,11]. Adsorption is one of the most adopted technologies for water treatment, thanks to a wide spectrum applicability in terms of both operational parameters and water properties [12]. Adsorption processes have gained crescent interest, showing high potential to be listed among the most efficient and cost-effective methods for the removal of contaminants from polluted waters [13]. Moreover, this process do not produce undesirable by-products and, if coupled with an effective regeneration process, it allows the recovery of the spent adsorbent [12,14]. Several different materials are commonly used as adsorbents such as zeolites, metal oxides, chitosan and activated carbons (ACs) [15–17]. Due to the general high cost of commercial materials, many efforts have been made in order to develop new adsorbent materials starting from by-products, for example, coal combustion fly ashes or scrap tires [18–20]. Focusing the attention on the removal of organic compounds such as benzene, alternative less expensive materials, such as modified montmorillonite [21] or ACs derived from agricultural by-products, sawdust and barks of *Arundo donax* L. stems [22], showed significant adsorption capacity, comparable with commercial adsorbents.

Adsorption processes are widely used both in *ex-situ* remediation techniques, such as pump and treat (P&T) [23], and in passive *in situ* techniques such as permeable reactive barriers (PRBs) [24,25]. In particular, PRB is a very promising groundwater remediation technique, which can be adopted also in case of multiple contaminations [26]. PRB technique consists in the insertion of a permeable wall into the contaminated aquifer, designed to intercept the whole polluted water flowing under the natural groundwater gradient. In this way, the contaminants are retained on the barrier and/or transformed into harmless substances, so to achieve a restoration of the aquifer [24]. Clogging phenomena due to salt precipitation is the main disadvantage of PRBs [27].

In recent years, several studies have been carried on the removal of benzene from contaminated groundwater via PRBs, in which benzene undergoes a series of degradation reactions, in case promoted by biological processes [28,29]. However, a very promising and innovative application of PRB makes use of an adsorbent material (e.g. activated carbon) as built material and it is commonly referred as permeable adsorptive barrier (PAB) [30]. Since adsorption process is currently adopted in the capture of benzene, the application of this process within PRB is expected to be very effective for the remediation of an aquifer contaminated by this hazardous compound.

In the present work, an innovative approach to design a PAB for the remediation of a contaminated aquifer is presented. A design procedure, formerly developed by the authors in a recent work [30], was implemented in COMSOL Multi-physics environment using a finite element model. A benzene-contaminated aquifer situated in North Naples (Italy), lately hit the headlines as "Gomorra's land", was taken as case study and *A. donax*-based activated carbon was considered as barrier built material [22]. Starting from a complete hydraulic characterization of the site, 2D simulations were carried out taking into account the specific dynamics of the aquifer under analysis and aimed at evaluating the optimal dimensions of a PAB (i.e. length, height and thickness), also allowing for long-term aquifer protection. Finally, the influence of hydrodynamic properties of the aquifer, such as hydraulic conductivity and longitudinal/transversal dispersivity, was evaluated via a sensitivity analysis.

2. PAB conceptual and mathematical model

A basilar step in modelling a PRB is the construction of a conceptual model, which includes the PRB characteristics (e.g. barrier dimensions, such as thickness, length and height, type of reactive material, position, etc.), the transport processes taking place in the aquifer and in the barrier, the mechanisms which govern the capture/transformation of the target pollutant and the relevant medium properties. A conceptual model is shown in Fig. 1, representing the main dimensions of a PRB, such as thickness, W_{PRB}, length, L_{PRB}, and height, H_{PRB}, and the distance from the contaminated plume, E.

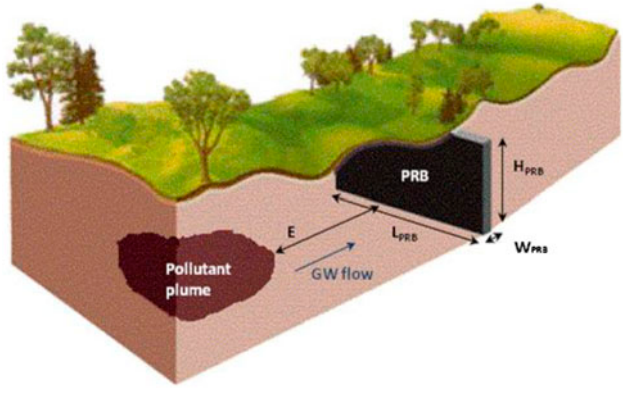

Fig. 1. PRB design conceptual model.

For an optimal design of the barrier, which allows the interception and the *in situ* treatment of the contaminated flow, a set of assumptions has to be respected [30,31]. In particular, the barrier has to be the closest possible to the pollutant plume, perpendicular to aquifer flow lines, and long, wide and thick enough to allow a thorough remediation of the plume, avoiding any polluted water overflow [31]. For these reasons, an important part of the PRB design process is the complete hydrogeological characterization of the aquifer and the determination of the plume characteristics and extension.

Furthermore, a mathematical model describing the groundwater flow and the transport of the contaminant has to be defined, also including the description of the geometry upon the conceptual geological model of the specific area. In this work, groundwater flow through a PRB and the transport phenomena describing the adsorption occurring inside the barrier were modelled using COMSOL Multi-physics.

The governing equation, which describes the fate and transport of pollutant into groundwater, can be written as follows [32,33]:

$$\frac{\partial(nC)}{\partial t} = -\overline{u}\nabla(nC) + \nabla(nD_h\nabla C) + R \tag{1}$$

The first, second and third terms on the right side of Eq. (1) indicate, respectively, the advection, dispersion and reaction terms. In Eq. (1), C represents the pollutant concentration in fluid, $\bar{u}$ the unit flux vector, n is the porosity and R is a pollutant source (positive) or sink (negative) term.

D_h is the hydrodynamic dispersion coefficient, expressed as follows [33,34]:

$$D_h = D + D_d{}^* \tag{2}$$

where D is the tensor of the mechanical dispersion and $D_d{}^*$ is the coefficient of molecular diffusion (a scalar). The components of the mechanical dispersion, D, may be expressed as follows [33]:

$$\begin{aligned} D_{xx} &= \alpha_x\frac{u^2}{U^2} + \alpha_y\frac{v^2}{U^2} \\ D_{xy} = D_{yx} &= (\alpha_x - \alpha_y)\frac{uv}{U^2} \\ D_{yy} &= \alpha_x\frac{u^2}{U^2} + \alpha_y\frac{v^2}{U^2} \end{aligned} \tag{3}$$

where D_{xx}, D_{xy}, D_{yx} and D_{yy} are all components of the dispersion tensor in a 2D system, u and v refer to the pore water velocity along the two direction axes (x and y), respectively, while α_x and α_y are the longitudinal and transverse dispersivity, and $U = \sqrt{u^2 + v^2}$. The transverse dispersivity is generally related to the longitudinal one by the following equation [34]:

$$\alpha_y = \alpha_x/10 \tag{4}$$

The unit flux vector $\bar{u}$ in Eq. (1) can be determined by the application of the Darcy equation, written as:

$$\overline{u} = -K_s \cdot \overline{\nabla}h \tag{5}$$

where K_s is the hydraulic conductivity and $\overline{\nabla}h$ is the hydraulic load gradient vector.

The third term on the right-hand side of Eq. (1) can be specified as:

$$R = -\rho_b\frac{\partial\omega}{\partial t} = k_c a[C - C^*(\omega)] \tag{6}$$

and describes the capture of the pollutant dissolved in water by the adsorbing material. In Eq. (6), ρ_b is the adsorbing material bulk density, k_c is the mass transfer coefficient for adsorption reaction, a is the external specific surface area of adsorbent particles and $C^*(\omega)$ is the pollutant concentration in the liquid phase at thermodynamic equilibrium with the concentration on the adsorbent solid. The latter can be obtained by an adsorption isotherm such as Langmuir model, expressed by the following equation:

$$\omega = \frac{\omega_{max}\ KC^*(\omega)}{1 + KC^*(\omega)} \tag{7}$$

where ω_{max} and K are the Langmuir parameters, generally obtained experimentally.

The boundary conditions assumed can be written as in the following:

$$\begin{aligned} &C = 0 \qquad \begin{bmatrix} x = 0 & \forall y\forall t \\ y = 0 & \forall x\forall t \\ y = Y & \forall x\forall t \end{bmatrix} \\ &\frac{\partial C}{\partial t} + \overline{u}\nabla C - \nabla(D_h\nabla C) = 0 \quad x = X \quad \forall y\forall t \end{aligned} \tag{8}$$

assuming a reference frame coinciding with the boundary of the domain, where X and Y are the size of the domain, respectively, in the x- and y-directions, and a constant porosity in all domain.

The numerical solution of Eqs. (1)–(7), with the related initial and boundary conditions (8), was performed by COMSOL Multi-physics, which accounted for both transport and the adsorbing phenomena occurring inside the aquifer and the PAB, in a unique framework. The initial concentrations in the liquid phase were assumed to be known (as reported in the following) and the initial benzene concentration onto the adsorbing material in the barrier was assumed to be zero.

The procedure followed to design the barrier required an iterative approach in order to evaluate the minimum barrier dimensions, in order to comply with the regulatory limit in the groundwater for the concentration downstream the barrier [30].

3. Site description

The case study examined a large area (2.25 km^2) in Giugliano in Campania, situated in the metropolitan area North Naples (Italy), where numerous solid waste landfills exist. The groundwater aquifer, located at a depth of 35–40 m from the land surface and confined by an aquitard (50 m), was found contaminated by a large number of pollutants, both inorganic and organic. Among these pollutants, benzene was detected at concentrations higher than the corresponding Italian regulatory limit for groundwater quality (C_{lim}), set at 1 μg L^{-1}. Soil composition of the area can be approximated to a single mineral (Neapolitan yellow tuff) whose hydraulic conductivity was found to assume variable values, namely $Ks_1 = 2 \times 10^{-5}$, $Ks_2 = 5 \times 10^{-5}$ and $Ks_3 = 1 \times 10^{-4}$ m s^{-1}. Similarly, the longitudinal dispersivity changes in the site assuming variable values $\alpha_{x1} = 0.5$ m, $\alpha_{x2} = 1$ m and $\alpha_{x3} = 4$ m [35–37]. The adsorption capacity for organic compounds of this material being very low [12,34], the initial solid concentration can be realistically assumed to be zero throughout the entire flow domain. The groundwater flow lines are east–west oriented, with piezometric groundwater levels ranging between 6 and 12 m a.s.l., under a piezometric gradient (J) of 0.01 mm^{-1} [30]. In Fig. 2, the benzene iso-concentrations in the actual conditions are reported, together with the map of the area and the piezometric groundwater levels.

Fig. 2 shows that benzene concentration changes in the area with a maximum of about 10 times higher than C_{lim}, set at 1 μg L^{-1}. The extension of the contaminated area is of about 500×450 m^2, with an average piezometric groundwater level of 8 m (where the plume is located). Once the volume of contaminated groundwater is identified, an *in situ* treatment represented by a PAB installation can be planned.

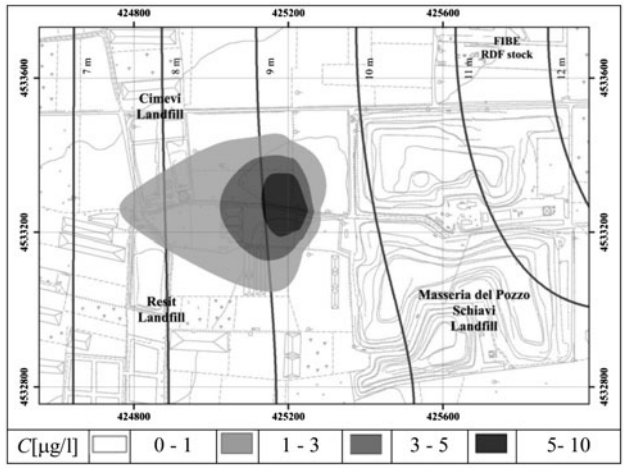

Fig. 2. Benzene iso-concentration contours and piezometric levels for the case study.

The solid used for the barrier set-up is an AC obtained from the stems of *A. donax* by H_3PO_4 acid activation, whose benzene adsorption capacity was reported in Basso and Cukierman [22]. The adsorption isotherm considered is described by the Langmuir model expressed by Eq. (7) and the values of the Langmuir parameters are equal to: $\omega_{max} = 35.1$ mg g^{-1} and $K = 0.0577$ L mg^{-1}.

In Table 1, the properties of the aquifer and the PAB parameters used in the numerical simulations are reported.

Values of the hydraulic conductivity and dispersivity were assumed as described in the following.

3.1. Sensitivity analysis

Because of the variation of some site parameters in the area, a sensitivity analysis was performed to evaluate the PAB properties deriving from their variability. In particular, the effect of hydraulic conductivity in the aquifer outside the barrier, K_S, and the longitudinal and transversal dispersivity, α_x and α_y were investigated. Values of transversal dispersivity were computed according to Eq. (4).

The barycentric case study considers a hydraulic conductivity Ks_2=: 5×10^{-5} m s^{-1}, and longitudinal, transversal and vertical dispersivity equal to $\alpha_{x2} = 1$ m and $\alpha_{y2} = 0.1$ m, respectively, corresponding to the Case 5 reported in Table 2 [26,30]. Starting from this set of parameters, for hydraulic conductivity and for each component of the dispersivity, a lower and a higher value were considered. All the values were combined according to the run plan reported in Table 2, in which nine simulation cases were defined.

Table 1
Case study: aquifer characteristic and numerical model parameters

Aquifer characteristic	
Polluted area total extent, A	0.225 km^2
Aquifer average piezometric level, H_w	8 m
Piezometric gradient, J	0.01 m m^{-1}
Porosity, n_s	0.25
Dry soil bulk density, ρ_s	1,400 kg m^{-3}
Hydraulic conductivity, Ks	2×10^{-5}–1×10^{-4} m s^{-1}
Longitudinal dispersivity, α_x	0.5–4 m
Transverse dispersivity, α_y	0.005–0.04 m
Molecular diffusion coefficient, D_d^*	10^{-8} m^2 s^{-1}
PAB characteristics	
Porosity, n_b	0.45
ACs bulk density, ρ_b	520 kg m^{-3}
Hydraulic conductivity, K_{PAB}	10^{-3} m s^{-1}
Longitudinal dispersivity, α_{xPAB}	0.05 m
Transverse dispersivity, α_{yPAB}	0.005 m
Molecular diffusion coefficient, D_d^*	10^{-8} m^2 s^{-1}
Ac BET surface area, S_{bet}	1.116 m^2 g^{-1}
Ac average pore diameter, Å	233.5 nm

Table 2
Simulation cases for the sensitivity analysis

	K [m s^{-1}]	α_x [m]	α_y [m]
Case 1	$Ks_1 = 2 \times 10^{-5}$	$\alpha_{x1} = 0.5$	$\alpha_{y1} = 0.05$
Case 2	$Ks_1 = 2 \times 10^{-5}$	$\alpha_{x2} = 1$	$\alpha_{y2} = 0.1$
Case 3	$Ks_1 = 2 \times 10^{-5}$	$\alpha_{x3} = 4$	$\alpha_{y3} = 0.4$
Case 4	$Ks_2 = 5 \times 10^{-5}$	$\alpha_{x1} = 0.5$	$\alpha_{y1} = 0.05$
Case 5	$Ks_2 = 5 \times 10^{-5}$	$\alpha_{x2} = 1$	$\alpha_{y2} = 0.1$
Case 6	$Ks_2 = 5 \times 10^{-5}$	$\alpha_{x3} = 4$	$\alpha_{y3} = 0.4$
Case 7	$Ks_3 = 1 \times 10^{-4}$	$\alpha_{x1} = 0.5$	$\alpha_{y1} = 0.05$
Case 8	$Ks_3 = 1 \times 10^{-4}$	$\alpha_{x2} = 1$	$\alpha_{y2} = 0.1$
Case 9	$Ks_3 = 1 \times 10^{-4}$	$\alpha_{x3} = 4$	$\alpha_{y3} = 0.4$

4. Results

The complete set of equations describing the complex phenomena occurring in the presence of the PAB was implemented in COMSOL Multi-physics and allowed the definition of all PAB parameters. A number of simulations were necessary in order to define the optimal set of parameters. The PAB resulted to be a continuous trench penetrating the aquifer at full-depth (50 m) up to the aquitard, at a distance, E, of 6 m from the pollutant plume and perpendicular to the groundwater flow with an orientation coincident with north direction; therefore, with an angle $m = 90^\circ$ with the groundwater flow direction. The height of the PAB, H_{PAB}, was set at 8 m in order to intercept the whole plume of polluted groundwater. For each of the nine cases analysed for the sensitivity analysis, the total length, L_{PAB}, and thickness, W_{PAB}, of the PAB were evaluated in correspondence of the most critical point S, i.e. the barrier point where the highest benzene concentration is reached during the run time. Fig. 3 reports the maximum benzene concentration in correspondence of the point S over the run time at the exit of the PAB, as a function of PAB thickness, W_{PAB}, varied from 0 m to 100 cm (assuming a $\Delta W = 10$ cm), for all the cases studied. For each case, the maximum benzene inlet concentration value was considered (i.e. the value corresponding to $W_{PAB} = 0$) and the regulatory limit (C_{lim}) was also indicated, in order to individuate the optimal thickness, W_{PAB}, as the value that assures a benzene concentration always lower than C_{lim}.

It is possible to observe that, even if the different parameters adopted (i.e. hydraulic conductivity and dispersivity components) determine differences in the maximum benzene inlet concentration (C values for $W_{PAB} = 0$), the optimal thickness value (W_{PAB}) results very slightly dependent on their variation. In Table 3, the optimal W_{PAB} values are reported, together with PAB length and, consequently, with the resulting overall PAB volume (V_{PAB}).

It can be concluded that only an increase in hydraulic conductivity can determine an appreciable increase in W_{PAB}, valuable in about 5 cm, and almost independently on the values assumed by the dispersivity components. However, it is worth to observe that these differences can be considered as negligible, because the realization of a PAB always includes a

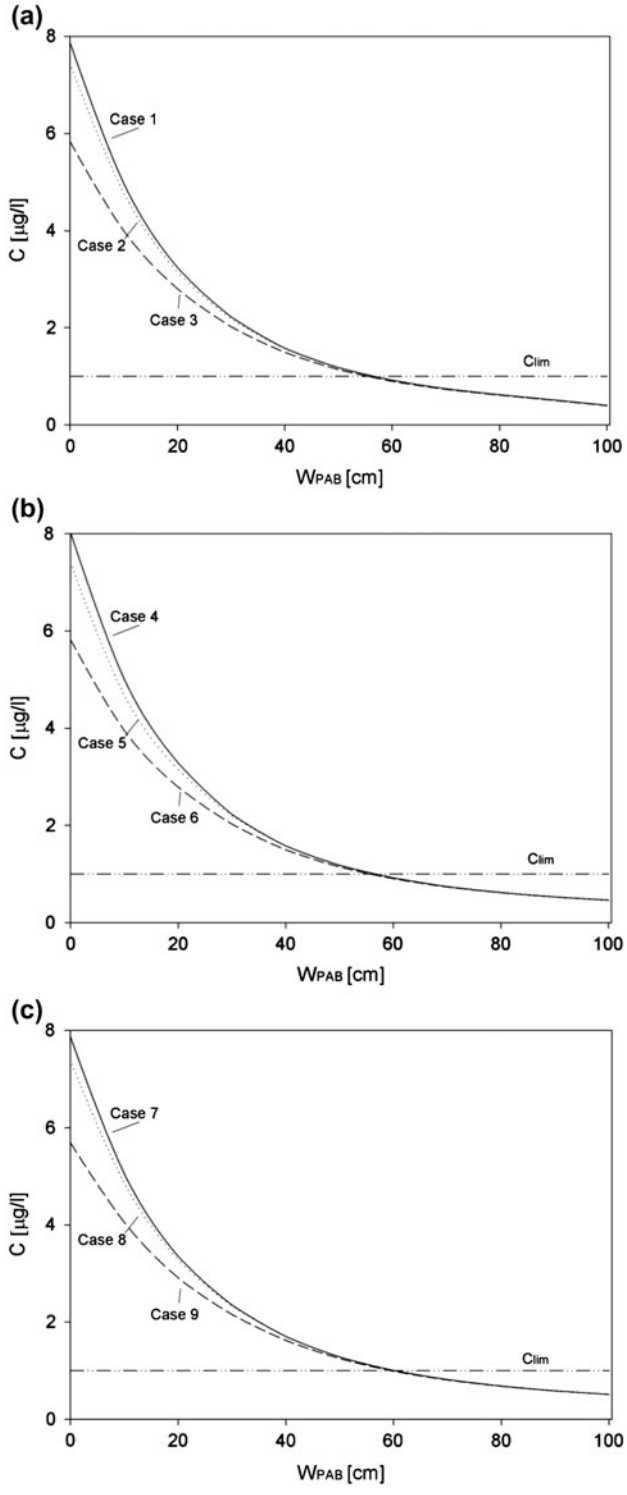

Fig. 3. Benzene concentrations of PAB at point S for different thickness values W_{PAB} (from 0 to 100 cm), respectively, for Cases 1–3 (a), Cases 4–6 (b) and Cases 7–9 (c).

Table 3
Optimal results for all cases analysed of the section S

	W_{PAB} [cm]	L_{PAB} [m]	V_{PAB} [m^3]
Case 1	56.70	400	1,814.40
Case 2	56.40	400	1,804.80
Case 3	55.40	390	1,728.48
Case 4	56.80	400	1,817.60
Case 5	57.00	400	1,824.00
Case 6	55.60	390	1,734.72
Case 7	60.40	400	1,932.80
Case 8	60.43	400	1,933.76
Case 9	59.50	390	1,856.40

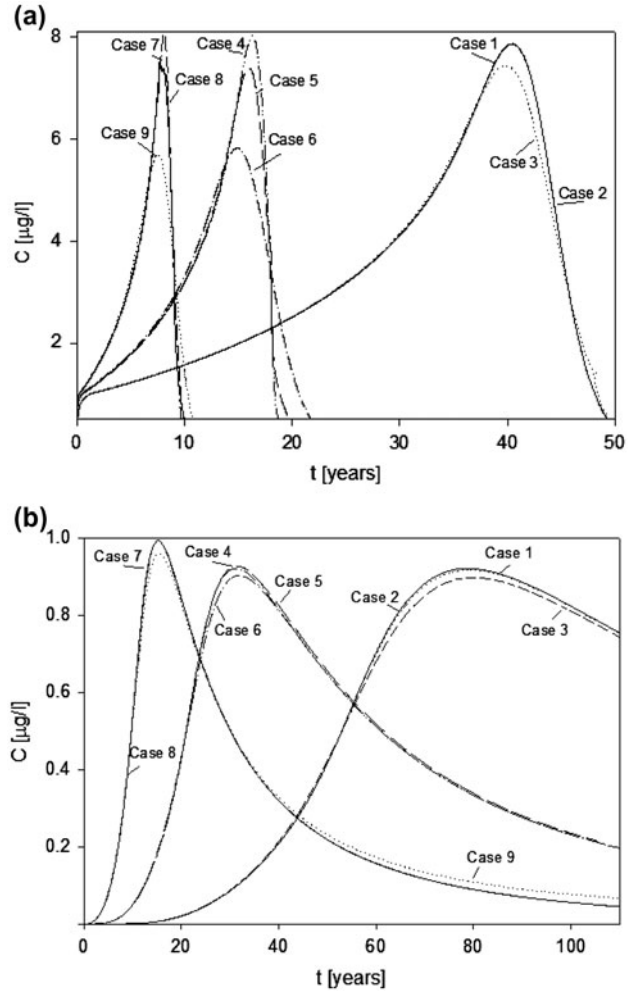

Fig. 4. Inlet (a) and outlet (b) benzene iso-concentrations of PAB at point S over the run time for all cases of sensitivity analysis.

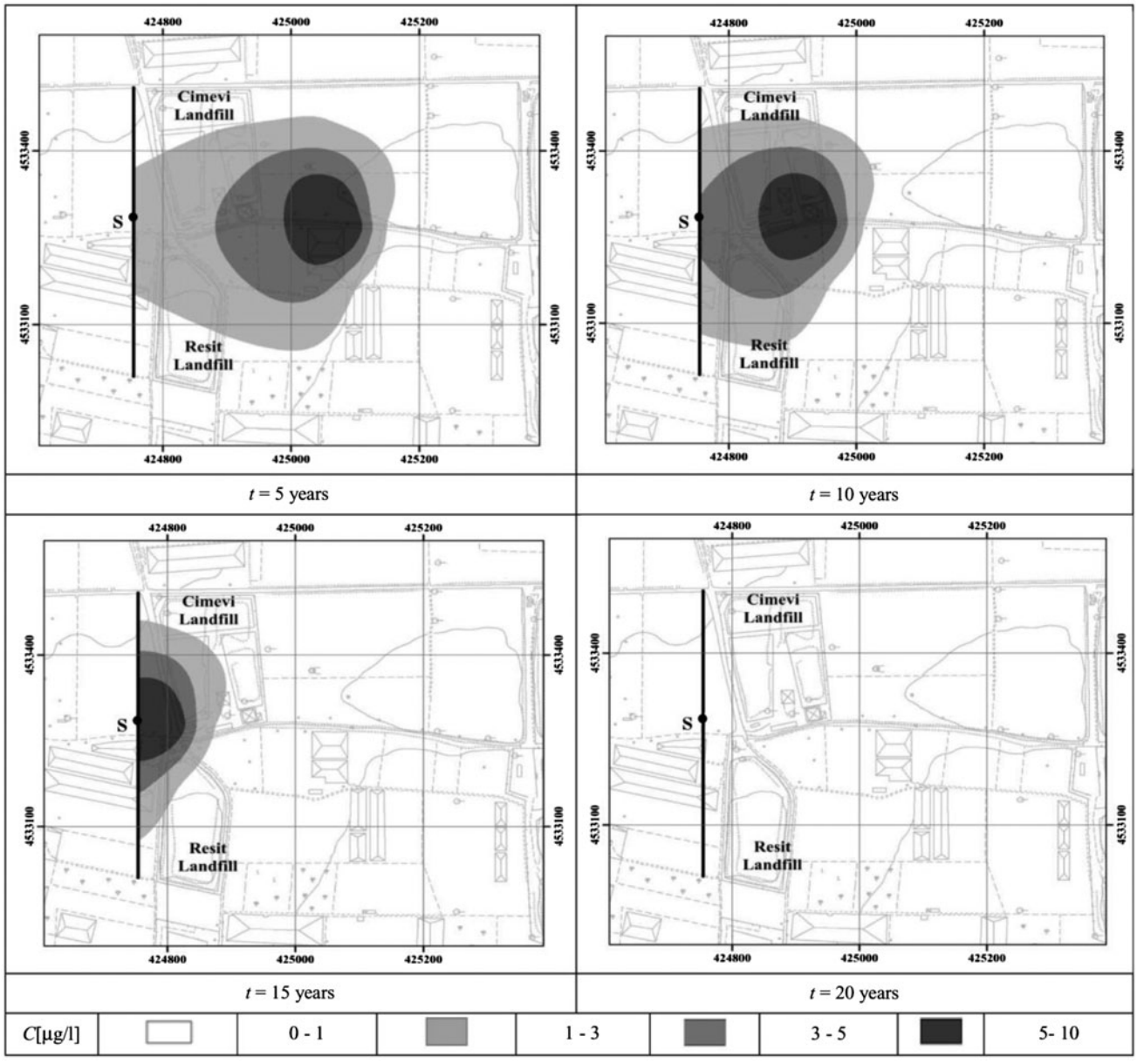

Fig. 5. Benzene iso-concentrations of PAB over the run time for Case 5.

safety factor, usually having magnitude higher than the differences in thickness previously determined.

The effectiveness of the thickness previously determined was verified during the entire run time by determining the outlet benzene concentration as a function of time at the most critical point S, for each of the simulated cases. The observation time was set at about 120 years and the results are depicted in the breakthrough curves reported in Fig. 4 both for inlet (a) and outlet (b) concentrations.

For all the simulated cases, the benzene outlet concentration was always lower than the regulation limit (set at 1 µg L^{-1}). Simultaneously, the effect of hydraulic conductivity and dispersivity can be highlighted in terms of concentration patterns, both for inlet and outlet concentrations. In fact, it is possible to observe that the peak in benzene concentration is shifted towards higher time when the hydraulic conductivity decreases. The effect of the components of dispersivity is less evident when the hydraulic concentration assumes the higher values among those investigated while it seems to be more influent in correspondence of the lowest value. However, as previously observed, the influence of these patterns on the PAB thickness

can be considered as negligible. The PAB designed for the case study was tested on the entire domain, adopting average values of hydraulic conductivity and dispersivity, according to the value reported in Table 2 (Case 5). To this aim, numerical simulations were carried out in order to determine the time evolution of the benzene contamination, starting from the initial condition reported in Fig. 2. An observation time of 20 years was set and the results were reported in Fig. 5 in the form of snapshots taken every five years.

Fig. 5 shows that pollutant spots move towards the barrier where they are captured; indeed in any run time, the benzene concentration flowing out of the barrier is confirmed to be always lower than the concentration limit. It can be concluded that after a lapse of time of 20 years, the aquifer is completely restored by benzene presence, this time strictly dependent on the hydraulic properties of the site (e.g. groundwater flux). Finally, the results show that the whole pollutant plume is intercept by the barrier, no overflow is observed at the barrier both sides and when the benzene inlet concentration decreases and possible desorption phenomena may occur, the barrier keeps its efficiency for a time longer than 100 years.

5. Conclusions

In this study, the efficacy of a PAB for the remediation of a benzene-contaminated aquifer was assessed. A 2D numerical model was developed and implemented in COMSOL Multi-physics environment using a finite element model to describe the pollutant transport in the aquifer and the adsorption on the PAB. The model was applied to a case study represented by a landfill in North Naples (Italy) in which a benzene contamination is present. An AC obtained from the stems of *A. donax*, whose BTEX adsorbing suitability was recently reported in the literature, was used as barrier adsorbing material.

The numerical simulations allowed the determination of the optimal barrier parameters in terms of position, distance from the pollutant plume and dimensions.

A sensitivity analysis was performed to evaluate the effects that uncertainties in some parameters, such as hydraulic conductivity and dispersivity, might have on PAB design. The results showed that the optimal barrier thickness is negligibly affected by a variation of those parameters within one order of magnitude, even if a slight effect on the time at which the highest benzene concentration peak reaches the barrier can be observed.

Finally, the effectiveness of the designed PAB was tested by determining the benzene outlet concentration on the entire analysed domain. The results showed that the outlet benzene concentration can always be maintained lower than the regulatory limit. In conclusion, PAB installation can be considered as a reliable way to reduce groundwater pollution and to assure the compliance with environmental prescriptions.

List of symbols

a	—	adsorbing material external surface area, $m^2\,m^{-3}$
C	—	liquid concentration, μg L^{-1}
C^*	—	equilibrium liquid concentration, μg L^{-1}
C_0	—	initial liquid concentration in batch experiments, μg L^{-1}
C_{in}	—	barrier inflow pollutant concentration, μg L^{-1}
C_{lim}	—	pollutant regulatory limit value, μg L^{-1}
C_{WPAB}	—	barrier outflow pollutant concentration, μg L^{-1}
D	—	tensor of mechanical dispersion
D_d^*.	—	molecular diffusion coefficient, $m^2\,s^{-1}$
D_h	—	hydrodynamic dispersion coefficient, $m^2\,s^{-1}$
X	—	distance between barrier and western boundary of the domain, m
Y	—	extension domain in y direction
H_{PAB}	—	barrier height, m
h	—	hydraulic load, m
A	—	polluted area total extent, km^2
E	—	distance between barrier and pollutant plume, m
J	—	piezometric gradient, $m\,m^{-1}$
K	—	langmuir constant, $l\,mol^{-1}$
K_s	—	hydraulic conductivity, $m\,s^{-1}$
K_{PAB}	—	barrier hydraulic conductivity, $m\,s^{-1}$
k_c	—	adsorption overall mass transfer coefficient, $m\,s^{-1}$
L_{PAB}	—	barrier length, m
n_b	—	barrier porosity
n_s	—	soil porosity
T	—	absolute temperature, K
u, v	—	groundwater flow velocity along (x and y), $m\,s^{-1}$
W_{PAB}	—	barrier thickness, m
V_{PAB}	—	barrier adsorbing volume, m^3
m	—	barrier orientation, °
α_x	—	longitudinal dispersivity, m
α_y	—	transversal dispersivity, m
α_{xPAB}	—	barrier longitudinal dispersivity, m
A_{yPAB}	—	barrier transversal dispersivity, m
Δx	—	horizontal space step, m
Δy	—	transversal space step, m
Δt	—	time step, d
ΔW	—	barrier thickness step, m
ρ_b	—	activated carbon bulk density, $kg\,m^{-3}$

ρ_s — dry soil bulk density, kg m^{-3}
ω — activated carbon adsorption capacity, mg g^{-1}
ω_{max} — maximum carbon adsorption capacity, mg g^{-1}
d_{pore} — activated carbon average pore diameter, A
S_{bet} — activated carbon BET surface area, m^2 g^{-1}

References

[1] P.J. Mouser, D.M. Rizzo, G.K. Druschel, S.E. Morales, N. Hayden, P. O'Grady, L. Stevens, Enhanced detection of groundwater contamination from a leaking waste disposal site by microbial community profiles, Wat. Resour. Res. 46 (2010) W12506 1–12.

[2] USEPA, Integrated Risk Information System—Benzene, 2003. Available from: http://cfpub.epa.gov/iris/quickview.cfm?substance_nmbr=0276.

[3] C.D. Phelps, L.Y. Young, Anaerobic biodegradation of BTEX and gasoline in various aquatic sediments, Biodegradation 10 (1999) 15–25.

[4] A.C. Frazer, P.W. Coschigano, L.Y. Young, Toluene metabolism under anaerobic conditions: A review, Anaerobe 1 (1995) 293–303.

[5] ATSDR, Toxicological Profile for Benzene, Agency for Toxic Substances and Disease Registry, Atlanta, GA, 2007. Available from: http://www.atsdr.cdc.gov/toxprofiles/tp3.html.

[6] C.A. Staples, A.F. Werner, T.J. Hoogheem, Assessment of priority pollutant concentrations in the United States using storet database, Environ. Toxicol. Chem. 4 (1985) 131–142.

[7] IPCS, Benzene, Environmental Health Criteria 150, World Health Organization/International Programme on Chemical Safety, Geneva, 1993. Available from: http://www.inchem.org/documents/ehc/ehc/ehc150.htm.

[8] D.W. Crawford, N.L. Bonnevie, R.J. Wenning, Sources of pollution and sediment contamination in Newark Bay, New Jersey, Ecotoxicol. Environ. Saf. 30 (1995) 85–100.

[9] Environment Agency, Review of the fate and transport of selected contaminants in the soil environment, Draft Technical Report P5–079/TR1, Environment Agency, Bristol, 2003.

[10] H.I. Chung, S.K. Kim, Y.S. Lee, J. Yu, Permeable reactive barrier using atomized slag material for treatment of contaminants from landfills, Geosci. J. 11 (2007) 137–145.

[11] E. Riser-Roberts, Remediation of Petroleum Contaminated Soils: Biological, Physical, and Chemical Processes, CRC Press, Boca Raton, FL, 1998.

[12] A. Erto, R. Andreozzi, F. Di Natale, A. Lancia, D. Musmarra, Experimental and statistical analysis of trichloroethylene adsorption onto activated carbon, Chem. Eng. J. 156 (2010) 353–359.

[13] A. Erto, A. Lancia, D. Musmarra, A real adsorbed solution theory model for competitive multicomponent liquid adsorption onto granular activated carbon, Microporous Mesoporous Mater. 154 (2012) 45–50.

[14] A. Erto, R. Andreozzi, A. Lancia, D. Musmarra, Factors affecting the adsorption of trichloroethylene onto activated carbons, Appl. Surf. Sci. 256 (2010) 5237–5242.

[15] S. Wang, Y. Peng, Natural zeolites as effective adsorbents in water and wastewater treatment, Chem. Eng. J. 156 (2010) 11–24.

[16] G. Crini, P.M. Badot, Application of chitosan, a natural aminopolysaccharide, for dye removal from aqueous solutions by adsorption processes using batch studies: A review of recent literature, Prog. Polym. Sci. 33 (2008) 399–447.

[17] F. Di Natale, A. Erto, A. Lancia, Desorption of arsenic from exhaust activated carbons used for water purification, J. Hazard. Mater. 260 (2013) 451–458.

[18] V. Leone, P. Iovino, S. Salvestrini, S. Capasso, Sorption of non-ionic organic pollutants onto a humic acids-zeolitic tuff adduct: Thermodynamic aspects, Chemosphere 95 (2014) 75–80.

[19] A. Molino, A. Erto, F. Di Natale, A. Donatelli, P. Iovane, D. Musmarra, Gasification of granulated scrap tires for the production of syn-gas and a low cost adsorbent for Cd(II) removal from waste waters, Ind. Eng. Chem. Res. 52(34) (2013) 12154–12160.

[20] A. Erto, L. Giraldo, A. Lancia, J.C. Moreno-Piraján, A low cost sorbent as an alternative to activated carbon for heavy metals adsorption, Water Air Soil Pollut. 224(4) (2013) 1531–1541.

[21] H. Nourmoradia, M. Nikaeena, M. Khiadani (Hajian), Removal of benzene, toluene, ethylbenzene and xylene (BTEX) from aqueous solutions by montmorillonite modified with nonionic surfactant: Equilibrium, kinetic and thermodynamic study, Chem. Eng. J. 191 (2013) 341–348.

[22] M.C. Basso, A.L. Cukierman, *Arundo donax*-based activated carbons for aqueous-phase adsorption of volatile organic compounds, Ind. Eng. Chem. Res. 44 (2005) 2091–2100.

[23] R.M. Cohen, J.W. Mercer, R.M. Greenwald, EPA Groundwater Issue, Design Guidelines for Conventional Pump-and-Treat Systems, EPA, 1998, 540/S-97/504. Available from: http://www.epa.gov/ada/issue.html.

[24] USEPA, Field Applications of In Situ Remediation Technologies: Permeable Reactive Barriers, EPA, 1999, 542-R-99-002. http://www.clu-in.org.

[25] I. Bortone, A. Di Nardo, M. Di Natale, A. Erto, D. Musmarra, G.F. Santonastaso, Remediation of an aquifer polluted with dissolved tetrachloroethylene by an array of wells filled with activated carbon, J. Hazard. Mater. 260 (2013) 914–920.

[26] A. Erto, I. Bortone, A. Di Nardo, M. Di Natale, D. Musmarra, Permeable Adsorptive Barrier (PAB) for the remediation of groundwater simultaneously contaminated by some chlorinated organic compounds, J. Environ. Manage. 140 (2014) 111–119.

[27] M. Prisciandaro, A. Lancia, D. Musmarra, Gypsum nucleation into sodium chloride solutions, AIChE J. 47 (2001) 929–934.

[28] C.H. Yeh, C.W. Lin, C.H. Wu, A permeable reactive barrier for the bioremediation of BTEX-contaminated groundwater: Microbial community distribution and removal efficiencies, J. Hazard. Mater. 178 (2010) 74–80.

[29] L. Chena, F. Liua, Y. Liub, H. Donga, P.J.S. Colbergc, Benzene and toluene biodegradation down gradient of a zero-valent iron permeable reactive barrier, J. Hazard. Mater. 188 (2011) 110–115.

[30] A. Erto, A. Lancia, I. Bortone, A. Di Nardo, M. Di Natale, D. Musmarra, A procedure to design a Permeable Adsorptive Barrier (PAB) for contaminated groundwater remediation, J. Environ. Manage. 92 (2011) 23–30.
[31] A.R. Gavaskar, Design and construction techniques for permeable reactive barriers, J. Hazard. Mater. 68 (1999) 41–71.
[32] J. Bear, Hydraulics of Groundwater, McGraw-Hill, New York, NY, 1979.
[33] L.F. Konikow, D.B. Grove, Derivation of Equations Describing Solute Transport isn Ground Water, US Geological Survey Water Resources Investigations, Denver, CO, 1977.
[34] L.W. Gelhar, C. Welty, K.R. Rehfeldt, A critical review of data on field-scale dispersion in aquifers, Water. Resour. Res. 28 (1992) 1955–1974.
[35] F. Bellucci, A. Corniello, R. De Riso, Geology and hydrogeology of the Somma-Vesuvio Volcano (Southern Italy), Memories of the XXIV Congress of IAH, Oslo, 1993.
[36] M.R. Boni, S. Sbaffoni, L. Tuccinardi, Performance of italian zeolitic tuffs and pozzolana in 2 chlorophenol removal from contaminated groundwater. Lab-scale experience, Brownfields IV, WIT Press, 2008, pp. 121–129.
[37] G. Aiello, A.G. Cicchella, V. Di Fiore, E. Marsella, New seismo-stratigraphic data of the Volturno Basin (northern Campania, Tyerrhenian margin, Southern Italy): Implication for tectono-stratigraphy of the Campania and Latium sedimentary basins, Annals of Geophysics 54 (2011) 256–283.